New Zealand Journal of Marine and Freshwater Research, 2013
http://dx.doi.org/10.1080/00288330.2013.778300

Taylor & Francis
Taylor & Francis Group

RESEARCH ARTICLE

The hydrodynamics of the southern basin of Tauranga Harbour

HW Tay[a]*, KR Bryan[a], WP de Lange[a] and CA Pilditch[b]

[a]*Department of Earth and Ocean Sciences, University of Waikato, Hamilton, New Zealand;* [b]*Department of Biological Sciences, University of Waikato, Hamilton, New Zealand*

(*Received 13 March 2012; accepted 30 January 2013*)

The circulation of the southern basin of Tauranga Harbour was simulated using a 3-D hydrodynamic model ELCOM. A 9-day field campaign in 1999 provided data on current velocity, temperature and salinity profiles at three stations within the main basin. The tidal wave changed most in amplitude and speed in the constricted entrances to channels, for example the M2 tide attenuated by 10% over 500 m at the main entrance, and only an additional 17% over the 15 km to the top of the southern basin. The modelled temperature was sensitive to wind mixing, particularly in tidal flat regions. Residence times ranged from 3 to 8 days, with higher residence times occurring in sub-estuaries with constricted mouths. The typical annual storm events were predicted to reduce the residence times by 24%–39% depending on season. Model scenarios of storm discharge events in the Wairoa River varying from 41.69 m^3/s to 175.9 m^3/s show that these events can cause salinity gradients across the harbour of up to 4 PSU.

Keywords: hydrodynamic model; salinity; temperature; residence times; circulation

Introduction

Estuaries are transition zones between land and sea and they transport and trap terrestrially-derived nutrients, sediment, contaminants and pollutants through the combined action of freshwater flow, wind, waves and tidal action (Hansen & Rattray 1966). Therefore, providing a detailed understanding of the hydrodynamics will ultimately give insights not only into the overall fate of terrestrial inputs, but also the exchange of sediments, pollutants, nutrients and also larvae between the estuary and the coastal seas. During transport, these can undergo alterations due to settling, chemical alterations and, in the case of larvae, growth and mortality that can change the seabed environment (e.g. morphology, sedimentation rate) and the composition of the overlying water column (e.g. oxygen and pH). The competing effects of vertical mixing and stratification control the distribution in the water column, and the availability of nutrients and oxygen to the benthic environment. Moreover, estuarine conditions can change during seasonal and episodic events from partially-mixed to well-mixed, causing periodic fluctuations which contribute to variations in turbulence and consequent changes in the stability of the water column, either promoting or suppressing biological and biogeochemical processes on the seabed. In many New Zealand estuaries the coastal effects from catchment development and navigation activities have resulted in increased sedimentation, heavy metal contamination, and catchment runoff (Chagué-Goff et al. 2000; Abrahim & Parker 2002; Oldman et al. 2009).

In New Zealand a wide variety of estuarine environments occur, such as drowned river valleys, barrier-enclosed estuaries, river mouth estuaries, estuaries resulting from tectonic activity and fjords which may be classified either

*Corresponding author. Email: yvonnethw@gmail.com

Table 1 Classification of estuaries in New Zealand based on hydrodynamic processes from Hume et al. (2007).

Category	Classification
A	Shallow basins, zero intertidal area, poorly flushed, wave suspension of sediments. e.g. coastal lakes
B	Elongate basins from several to 10 m depth, majority subtidal, river-dominated flow, well-flushed, bars at ocean side of estuary entrance, minor wind fetch and small wave, muddy sediments in areas of high tidal flows. e.g. tidal river mouths
C	Mouth of main river channel connects to lagoons, significant intertidal area, river-dominated flows, well-flushed river channel and poorly-flushed lagoon, minor wind fetch and wave resuspension e.g. tidal river mouths
D	Shallow, circular to elongate basin and wide entrances that open to ocean, subtidal with intertidal areas restricted to sheltered areas, little river influence, ocean forced circulation, wave-driven sedimentation, sandy substrate e.g. coastal embayments
E	Shallow, circular to slightly elongate basins, extensive intertidal area, narrow entrance, ebb and flood tidal deltas at the mouth on littoral drift shores, ocean forced circulation, strong flushing and wind mixing, sandy substrate e.g. tidal lagoons or barrier-enclosed lagoons
F	Shallow and narrow basins, deep channels leading off the main basin, tide-dominated, less pronounced than E in mixing and wave resuspension, sandy substrate with transition to muddy substrate in upper portion of the arms, well-mixed in main basin but upper reaches of arms are characterised by stratification and salt wedges e.g. barrier-enclosed lagoons or drowned river valleys
G	Deep, narrow, elongate, largely subtidal basin, characterised by sills at the mouth, thermohaline forcing, poor flushing e.g. fjords or sounds
H	Deep, narrow, elongate basins, largely subtidal, thermohaline forcing, longitudinal gradient (head to mouth) with riverine forcing and stratification in the headwaters, and ocean forcing and vertical mixing at the entrance, poor flushing, fine sand or mud substrate e.g. sounds, drowned valleys, rias or fjords

by physiography or salinity structure (Healy & Kirk 1992). Recently, Hume et al. (2007) provided a controlling factor classification of New Zealand estuaries (Table 1), based on broad scale physical components (e.g. climate, oceanic and riverine conditions, catchment characteristics). Based on Hume et al.'s (2007) level 2 classification for estuary hydrodynamic processes, the northwest coast estuaries are generally categories B and C, which means that the river volume is greater than the tidal volume entering the estuary. In contrast, northeast coast estuaries are generally categories D, E and F, where there is little river influence and they are relatively shallow. In the southeast and west of the North Island, the estuaries are generally category B (Table 1).

Tauranga Harbour (Fig. 1) is one of the largest estuaries in New Zealand, and forms a particularly important case for detailed study because it is a zone of conflict associated with a wide range of catchment and estuarine-based activities. It is a barrier-enclosed mesotidal estuarine lagoon (Davies-Colley & Healy 1978), corresponding to a category F estuary according to Hume et al. (2007). Approximately 64 (14%)

of New Zealand estuaries fall into this category. These types of estuaries are generally shallow and contain extensive intertidal flats, and have always been assumed to be vertically well-mixed and well-flushed (Healy & Kirk 1992; Tay et al. 2012), thus minimising the risks associated with stratification and hypoxia (Rabouille et al. 2008). Commercial development is centred within the southern basin, which is the site for the country's largest export port, Port of Tauranga. Like most urban waterways, Tauranga Harbour has had to accommodate the increase in commercial shipping associated with the port, combined with the growing population in the sub-catchments surrounding the harbour, who want marinas and easy access to the coast. Such multiple uses are not always consistent with the predevelopment ecology of this otherwise mangrove- and seagrass-lined habitat, which is well known for its shellfish beds (Cole et al. 2000; Scholes et al. 2009).

A sound understanding of the hydrodynamic drivers is needed to predict the impact of these developments and thus inform management plans that aim to maintain the health of the estuarine system. Key parameters that underpin such plans are: 1) the residual circulation patterns, which can be large in shallow, wide estuaries; 2) residence times; and 3) the vertical structure. To date, investigations of the hydrodynamics of Tauranga Harbour have mostly concentrated on the port's main navigation channels in order to assess the impacts of development (Vennell 2006; Spiers et al. 2009). An unpublished 1983 study commissioned by Bay of Plenty Harbour Board did investigate the hydrodynamics of the entire harbour, although its primary focus was future port and roading development (Black 1984; Barnett 1985; Healy 1985). It comprised a major field campaign, a hydrodynamic and sediment transport model, and a morphological study (Healy et al. 1987, 1993). Another unpublished 3-D numerical modelling study was undertaken by the National Institute of Water and Atmospheric Research (NIWA) as part of the sedimentation study commissioned by Environment Bay of Plenty in 2009 (now Bay of Plenty Regional Council [BOPRC]). However, despite the number of large investigations and smaller thesis studies on the area, none have characterised the salinity and temperature structure in the southern basin of Tauranga Harbour. Moreover, the hydrodynamic and circulation studies that exist are not readily accessible.

This paper describes key features of the tidal and wind-induced circulation within the southern basin of Tauranga Harbour, combining results from both a comprehensive field programme and implementation of a 3-D hydrodynamic model. A calibrated numerical model of harbour dynamics offers information over greater spatial and temporal scales and resolutions than instrument deployments can provide. The role of the field data was to assist in calibration and validation of the hydrodynamic model. The model provided spatial and temporal information on tides and currents, and characterised the influence of wind on circulation patterns during typical fair weather and storm conditions. It also delimited the influence of Wairoa River discharge on the salinity–temperature patterns in the harbour. The numerical model enables the influences of a variety of changes to the forcing such as wind and freshwater discharge events to be isolated and resolved. Although the results are specific to Tauranga Harbour, the harbour's shallow intertidal morphology, characterised by constricted entrances, is typical of many in New Zealand (Hume et al. 2007).

Methods

Field site description

The barrier-enclosed estuarine lagoon of Tauranga Harbour (Fig. 1) is impounded by two Holocene barrier tombolos, Mt Maunganui for the Tauranga (southern) basin, Bowentown for the Katikati (northern) basin, and a 24-km long sand barrier Matakana Island (Davies-Colley & Healy 1978). The two basins are connected, albeit with a large tidal flat separating them, and, following past studies on the harbour (Barnett 1985; de Lange 1988, Tay et al. 2012),

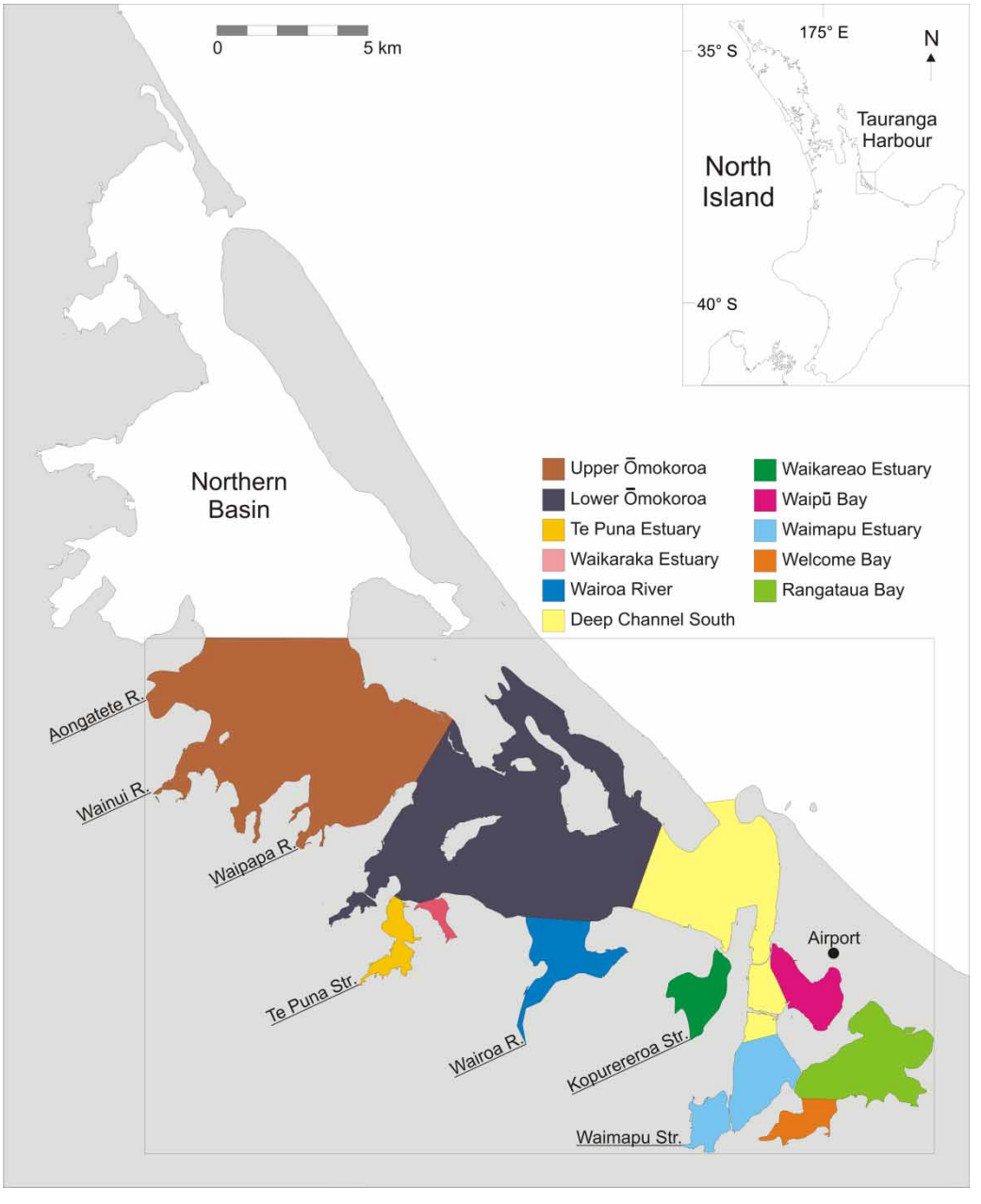

Figure 1 Location map of the study area in the southern basin of Tauranga Harbour. The box outlines the extent of the model grid. The harbour is subdivided into different regions based Hume et al. (2009) to classify residence times. The river and stream inflow boundaries are marked and named.

we assume that there is little or no exchange of water between each. Therefore, only the southern basin is simulated in this study (area at mean sea level: 95×106 m^2; volume at mean sea level: 174×106 m^3). The harbour has large tidal flat regions (41 km^2), which are exposed during

periods of low tide and a spring tidal range of 2 m (Heath 1976). The Wairoa River is the main freshwater input into the harbour with a mean inflow of 17.6 m^3/s (Park 2004).

Data collection

A 9-day field campaign was undertaken from 3–11 February 1999 to obtain data for calibration of the numerical model. Three InterOcean S4 electromagnetic current meters were deployed over four tidal cycles along transects at Ōmokoroa (3–5 February 1999), Motuhou (6–8 February 1999) and Western sites (9–11 February 1999) (Fig. 2) to determine tidal elevation, current velocity, salinity and water temperature. Only one of the S4 current meters deployed along each transect had sensors for water depth, salinity and temperature. Conductivity, temperature and depth (CTD) casts were also taken at each station using a Seabird Electronics CTD. In addition, unpublished CTD measurements taken previously (Giles 2002) at Ōmokoroa and near the entrance of the main harbour at approximately high tide every 2 weeks for a year in 2001 were used for validation of the modelled salinity patterns. To validate modelled current speeds we used datasets of longer duration. This included: ADCP current meter data collected in 2008 by the Port of Tauranga at the harbour entrance (A on Fig. 2); Falmouth Scientific Instrument (FSI) current and water level recorders (F1 and F2 on Fig. 2) deployed from 10 May 2006 to 8 June 2006 by Spiers et al. (2009); and water level measurements from the

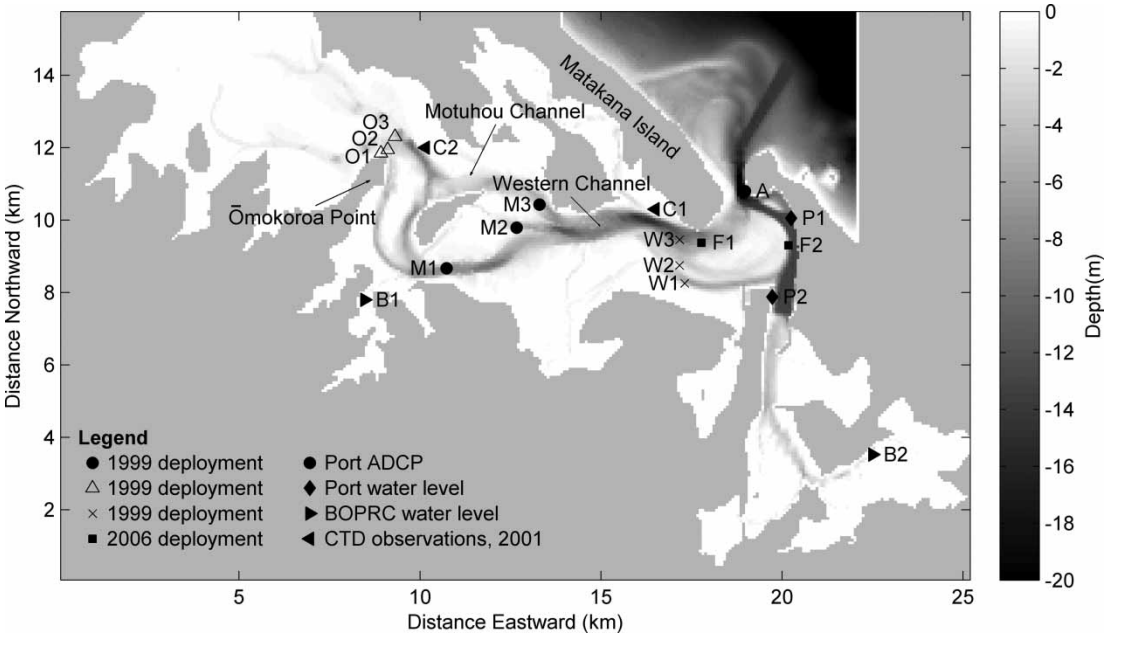

Figure 2 Site map of the location of the 3 November 1999–11 November 1999 S4 current meter deployments at 'Ōmokoroa (O1, O2, O3)', 'Motuhou (M1, M2, M3)' and 'Western (W1, W2, W3)' which were used for model calibration. C1 and C2 mark the location of CTD deployments at Ōmokoroa and Western respectively in 2001. F1 and F2 mark the locations of the 10 May 2006–8 June 2006 FSI current meter deployments. P1 and P2 mark the Port of Tauranga and B1 and B2 mark the Bay of Plenty Regional Council water level recorders used for the 2006 validation runs. The location of the ADCP current meter is marked as A, which was used for additional validation. The ELCOM bathymetry grid is plotted as the background to the site map.

same period collected by the Port of Tauranga (P1 and P2 in Fig. 2) and BOPRC (B1 and B2 on Fig. 2).

Model description and set-up

The Estuary, Lake and Coastal Ocean Model (ELCOM) is a 3-D hydrodynamic model (Hodges et al. 2000; Hodges & Dallimore 2006) used for predicting velocity, salinity and temperature distribution in water bodies. The ELCOM model used in the present study is based on the unsteady Reynolds-averaged, hydrostatic Boussinesq, Navier-Stokes and scalar transport equations (Hodges et al. 2000), and includes modelling of density-driven flows. The model uses Chezy-Manning bottom stress to simulate dissipation over the whole water column. Vertical mixing is simulated with a 1-D mixed-layer model in each level, from which turbulent kinetic energy is extracted and transported with the 3-D model. More details of the mixing models can be found in Hodges et al. (2000). Water level conditions along the open ocean boundary of the model domain were derived from NIWA tidal model (www.niwa.co.nz/our-services/online-services/tides). The tidal constituents used in the NIWA tidal model are M2, S2, N2, K2, K1, P1, Q1 and O1. Unfortunately, there are very few measurements of shelf salinity variations within the Bay of Plenty. Therefore, open boundary salinity was derived from four offshore transects carried out between October 2003 and May 2004 (Park 2005). For each transect, sea surface salinity (< 20 m depth) was extracted, averaged and interpolated between the 4 days of measurements to provide an estimate of seasonal changes in salinity. We assume that the offshore salinity structure in February 1999 was the same as in February 2004, although it may be affected by interannual variations induced by the El Niño–Southern Oscillation (ENSO). However, the period when the offshore transect was collected was neither a strong La Niña nor El Niño event.

BOPRC maintains a wave buoy 13 km offshore of Pukehina Beach (37.411°S, 176.371°E). The wave buoy measures wave and temperature conditions every 20 minutes. As the wave buoy was first deployed in April 2002, temperature measured by the wave buoy in February 2008 was used for the model as it was the only available summer data provided by the council. Both 1999 and 2008 were La Niña years, with an air temperature difference of 0.2 °C (the mean February temperature for 1999 and 2008 was 19.7 °C and 19.5 °C respectively). The El Niño in 2006 did not begin until the end of the year, and so should also be comparable. Weather data (wind, air temperature, relative humidity, solar radiation, atmospheric pressure and rainfall) for this study were collected by the Tauranga Aero automatic weather station (AWS) located at Tauranga Airport (Fig. 1). These data were obtained from the NIWA CliFlo database.

The freshwater inflow boundaries into the southern basin of the harbour are Wairoa River, Waipapa River, Waimapu Stream, Kopurereroa Stream, Te Puna Stream, Wainui River and Aongatete River (Fig. 1). The inflow rate of rivers and streams were sourced from BOPRC's monitoring data archives. BOPRC monitoring provided continuous flow data for Wairoa River, Waipapa River, Waimapu Stream and Kopurereroa Stream. For Wainui and Aongatete rivers, the inflow records were sparse, hence a design hydrograph for each river was created based on the empirical model in the US Soil Conservation Service handbook (SCS 1972, 1975). For the ungauged Te Puna Stream, a design hydrograph was also created to estimate the stream discharge using the SCS (1972, 1975) approach that was adapted to similar catchments in the Auckland region (Beca Carter Hollings and Ferner Ltd 1999). As there were only sparse measurements of water temperature for streams and rivers in the harbour, the model water temperature for the rivers and streams was estimated from the air temperature at Tauranga Airport. Groundwater inflow was not included in the model.

A number of sources were used to construct the model bathymetry. Single-beam and some multi-beam echosounder surveys collected by the

University of Waikato were used in tidal channels (see Spiers et al. 2009). Data for the rest of the harbour were obtained from a combination of hydrographic soundings around the port area (provided from the Port of Tauranga and the Tauranga Harbour Board) and digitised from the navy fairsheets outside of the port region. The original fairsheets were from 1983 and tidal channel bathymetry was surveyed in the late 1990s by the Port of Tauranga. All data were standardised to New Zealand map grid coordinates and reduced to Tauranga chart datum. Figure 2 shows the bathymetric grid (75×75 m resolution) of the southern basin of Tauranga Harbour used in the ELCOM modelling. The model had 12 vertical layers with thicknesses varying between 0.5 m near the surface and 5 m near the seabed. The 'calibration simulations' were performed for the period 3–11 February 1999 when field data were collected. The 'validation simulations' were selected to coincide with the FSI deployment in 2006 and the ADCP observations in 2008. Due to all simulations beginning from a cold start (i.e. flat water, and no currents), a period of 3 days (six tidal cycles) was allowed for the model to 'spin up' before model results were extracted. The temperature and salinity initial conditions were spatially varying as it takes many days of model time to establish an equilibrium salinity and temperature distribution. The model flow speeds and amplitudes were calibrated by adjustment of the bottom drag coefficient within physically-reasonable limits to find the smallest root mean square error between modelled and measured data. The optimal drag coefficient varied with location in the harbour, so a varying bottom drag coefficient was applied across the model domain with bottom friction set higher (more friction) in channel areas and a lower (reduced bottom friction) in the tidal flat areas. Data were extracted from model output for Ōmokoroa, Motuhou and Western stations to compare with measured field data.

Temperature and salinity were not calibrated because data–model mismatches were likely more due to assumptions made in determining the temperature and salinity characteristics of the boundary and input conditions, rather than the way in which heat and salt are modelled in ELCOM. Modelled temperature and salinity variations were directly compared to the observations from the CTD deployments undertaken during the 9-day field campaign in February 1999. The field campaign was conducted in summer conditions when river input was at its lowest. In lieu of validation, and in order to determine how well ELCOM performed over a wider range of freshwater input conditions, three Wairoa discharge 'events' were modelled for 10 December 2007 (41.69 m^3/s), 16 August 2008 (63.69 m^3/s) and 8 September 2008 (175.9 m^3/s), and the output was compared to salinity variations measured biweekly during 2001. Given that the events modelled were different than the measured events, and that the observations were not targeted around events, comparison was made by examining the modelled and observed relationship between the salinity difference across the two stations and the discharge in the Wairoa River.

Scenarios were developed to investigate the environmental controls on circulation patterns in the harbour (summarised in Table 2). The scenarios were simulated for February 2008, unless stated otherwise in the text, due to the availability of offshore water temperature data

Table 2 Description of different model scenarios applied to southern basin of Tauranga Harbour.

Scenario	Description
0	Base case (current wind condition)
1	Wind conditions 'switched off'
2	Storm wind (11 m/s) from 100 degrees in winter
3	Storm wind (11 m/s) from 100 degrees in summer
4	Storm wind (11 m/s) from 230 degrees in winter
5	Storm wind (11 m/s) from 230 degrees in summer
6	High freshwater discharge from Wairoa River (540 m^3/s)

measured by the wave buoy. The base case (scenario 0) was simulated with measured wind conditions. In scenario 1, the wind conditions were 'switched off' in order to examine the effect of wind on circulation patterns in the southern basin. For residence time comparisons, the harbour was divided into sub-regions corresponding to those defined by NIWA in its investigation of harbour sedimentation patterns (Hume et al. 2009; Fig. 2). Examination of 17 years of wind records from Tauranga Airport indicated that the conditions in February 2008 (wind speed 3.3 m/s, wind direction 190 degrees) were typical of Tauranga, with the wind speed having a 2.3-day return period. In addition to this, the 1-year wind event (11 m/s) was also modelled using the most common direction (230 degrees) and the next most common direction (100 degrees). This was done for both winter and summer conditions (scenarios 2–5). In scenario 6, the effect of a high freshwater discharge event from the Wairoa River (c. 540 m^3/s), which is the main freshwater inflow into Tauranga Harbour (with a mean freshwater inflow of 17.6 m^3/s [Park 2004]) was simulated. The modelling contrasts a period when the extreme flooding event occurred (15 April 2008) with a period of similar tidal and wind conditions. but with normal flow conditions in the Wairoa River (1 April 2008).

Results and discussion

Current speed and water level calibration and validation

The model was calibrated by adjustment of bottom drag coefficient (BDC) within the range 0.001 to 0.02 (the 'calibration simulations'). The root mean square (RMS) error between modelled and measured data (not shown) were used to find the best results which was a depth-varying BDC being 0.01 in areas deeper than 1 m and 0.005 in areas less than 1 m deep. Figure 3 illustrates time-series of measured and modelled data for the sampling period (9–11 February 1999) at station 1 at the Western site. Simulation results for the Western site are in good agreement with the measured data. Tidal elevation was generally consistent (RMS error between 0.14–0.2 m; Table A1.1) as was current speed (RMS error between 0.08–0.15 m/s; Table A2.1). Model calibration for current speed and direction (Fig. 3) was generally good, with the general trend better represented for incoming water (absolute difference of 0.01–0.04 m/s [4.2%–7.5%]) compared to the outgoing water (absolute difference of 0.08 to 0.1 m/s [14%–22%]). The mean absolute error (MAE) was sometimes greater when the model did not exactly capture the timing of the change from flood to ebb tide (Table A2.1).

The model was also calibrated against the eight other stations (locations shown in Fig. 2). Simulation results for the other stations at Ōmokoroa, Motuhou and Western are in good agreement with the measured data (not shown, results summarised in Tables A1.1 and A2.1). The match between modelled and measured tidal elevation at Ōmokoroa and Motuhou (Table A1.1) was generally consistent (RMS error between 0.18–0.24 m). Model current speed and direction was better represented for incoming water (relative difference of 2%–20%) compared to outgoing water (relative difference of 14%–37.5%) across all stations except at Ōmokoroa station 1. At Ōmokoroa station 1, the simulated incoming tide was over-predicted by 0.3 m/s (percentage error of 50%). The direction for measured S4 data from Ōmokoroa was noisy and the speed was low, suggesting that the lack of fit here may be due to an eddy around the Ōmokoroa headland that was not resolved by the model. At Ōmokoroa station 2, the simulated speeds for outgoing tide were under-predicted by 0.2–0.3 m/s (percentage error of 25%–37.5%). At Motuhou stations 2 and 3 and Western station 2, the simulated current speed for outgoing tide was under-predicted by 0.2 m/s (percentage error of 33%–50%). Finally, the model was also validated against ADCP data collected at the mouth of the harbour by the Port of Tauranga (Fig. 4) and FSI current meter data (the 'validation simulations'). ADCP data were

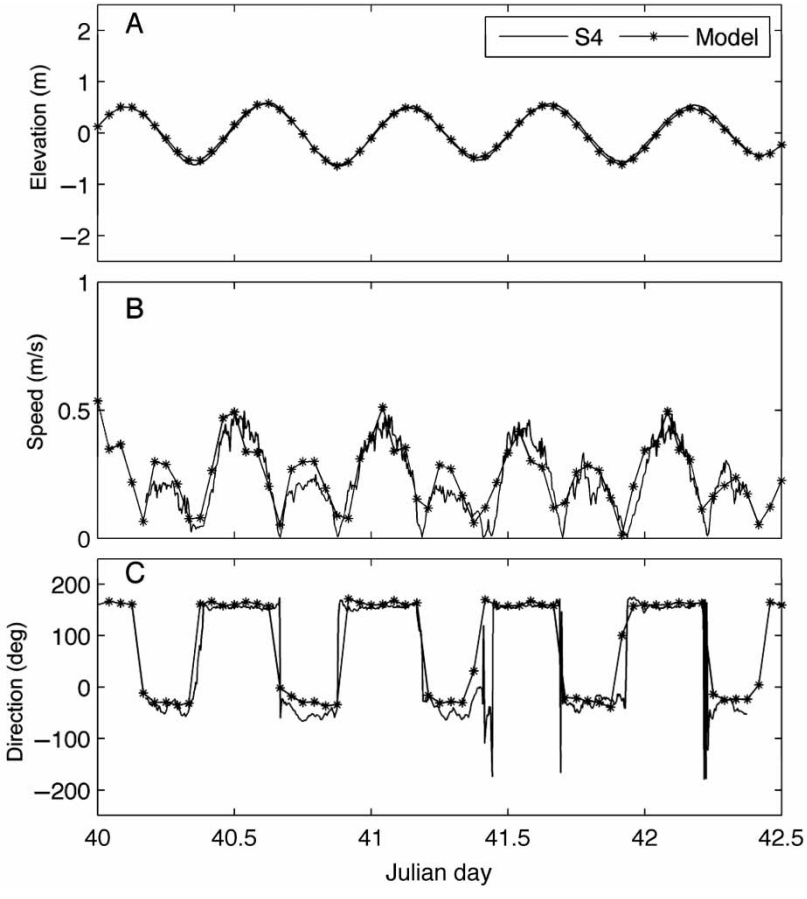

Figure 3 Model calibration: modelled elevation (A), speed (B) and direction (C) plotted with S4 current meter observations for measurements at station 1 on the Western transect (W1 in Figure 2) in the southern basin of Tauranga Harbour.

not provided for 1999, and so observations for 2008 were used (which were the simulations also used for the scenarios). Both these comparisons yielded consistent results, with a 0.12–0.18 m/s RMS error (which was a 20%–40% error).

Tidal variations

Tidal constituents were extracted from the model and observations using a freeware tidal harmonic analysis package (T-TIDE written by R. Pawlowicz [Pawlowicz et al. 2002]). For the 2006 validation runs, the model and observations were both dominated by the M2 tide (c. 0.66 m), with the S2, N2 and K1 contributing approximately equally to the remaining signal (c. 0.07 m). The O1 tide contributed about 0.015 m, and the other components were much smaller or unresolvable with the month-long deployment. The model under-predicted the M2 tide by about 0.03 m, and over-predicted the S2, N2 and K1 tides by 0.02 m, 0.02 m and 0.04 m respectively (summarised in Table A1.1). When we forced our model with water level observations from the Moturiki tide gauge near the entrance of the harbour (provided by NIWA for the validation period), the modelled

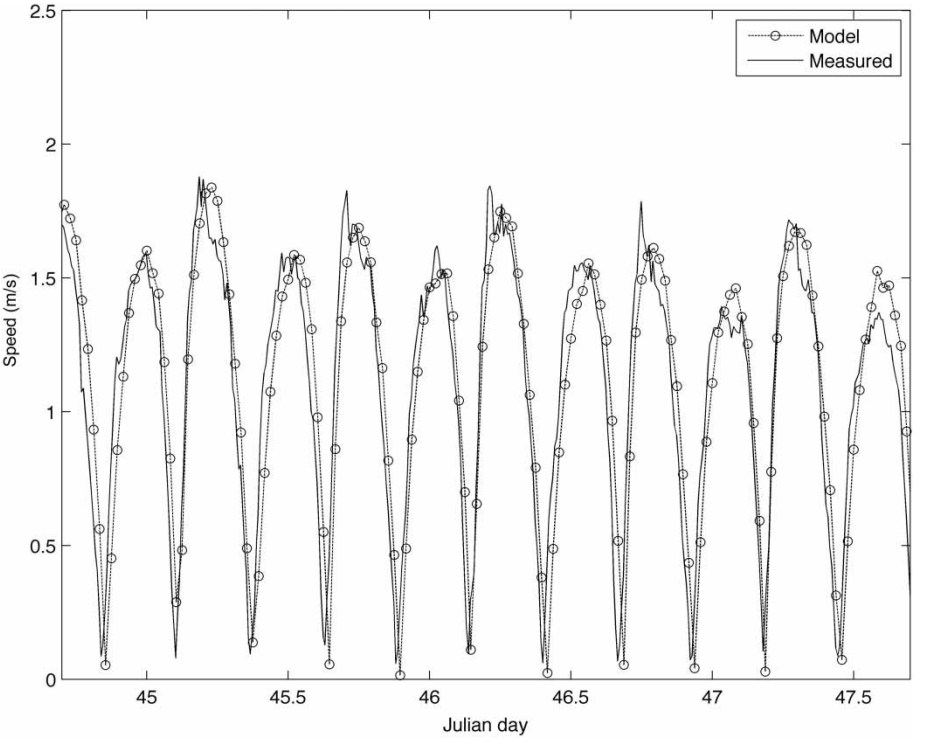

Figure 4 Model validation: comparison between 2008 measured (ADCP data) and modelled current speed at the mouth of the harbour (point A on Figure 2).

amplitude predictions for constituents M2, K1, N2 and S2 for output at locations K1, K2, P1 and P2 are much more accurate (< 0.01 m different than observed). It may be that the differences obtained between the model forced using the NIWA tidal model and the model forced using measured water level recordings at Moturiki may be due to unusually small tides during the verification period. Tidal harmonic analysis of Moturiki observations and observations at the two port water level recorders by Mathew (1997) for 1989–1995 indicate that the M2 tide is normally around 0.73 m. Phases were predicted well near the entrance, but at higher reaches in the harbour the phase error could reach 8 degrees (the modelled tide is 25 minutes too early) on the M2 tide.

For the dominant tidal harmonic constituents for Tauranga Harbour, the M2 and S2 tides, the amplitude and phase were extracted using a 5-year model run (for 2006–2010) at every location throughout the model grid in order to study the spatial variation of the amplitude and phase. Longer model runs are needed to provide realistic estimates of constituents, as these vary from year to year in the harbour (Mathew 1997). The model run was forced using water levels from the NIWA tidal model on the outer boundary. Creating the many freshwater and climatic forcing datasets needed for the entire 5-year period would be time-consuming, so the conditions that occurred during 2006 were used during the subsequent four years. The amplitude of the dominant M2 tidal constituent was attenuated from 0.73 m to 0.7 m (4%) as it propagated over the short distance (c. 500 m) through the main harbour entrance as the tidal flow is constricted through

the narrow entrance (Fig. 5A). The M2 amplitudes at P1 and P2 compare to within 0.01 m with those reported in Mathew (1997) at the same sites, indicating that forcing our model with the NIWA tidal model provides generally reliable predictions within the harbour (and the larger errors reported for the validation period in 2006 were anomalous). The tidal amplitude

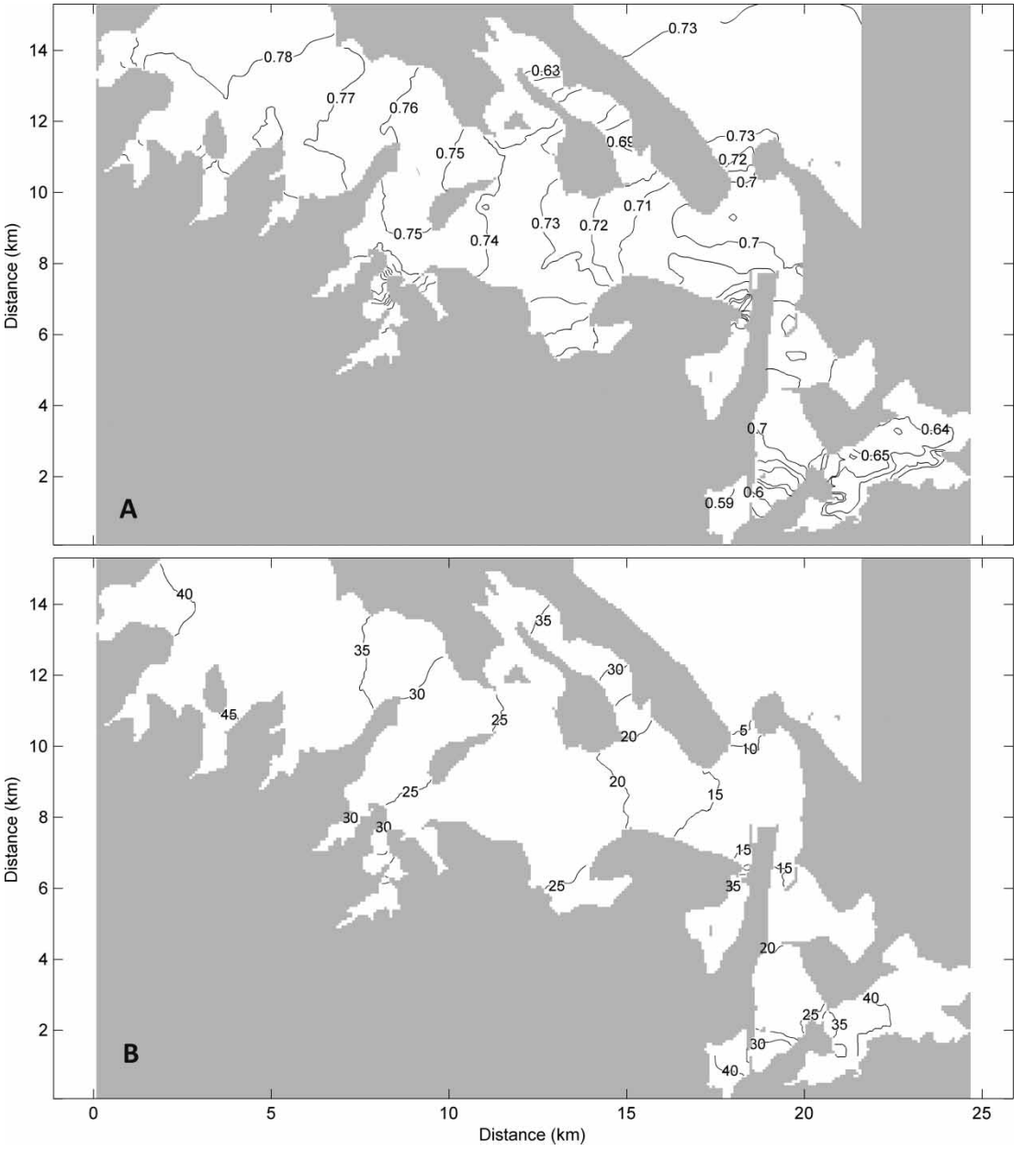

Figure 5 Panel A: M2 cotidal diagram of amplitude (m). Panel B: M2 cotidal diagram of phase (degrees) extracted from output of a 5-year model run. These simulations were forced on the outer boundary with output from the NIWA tidal model, and the M2 component extracted using tidal harmonic analysis software (see text).

stayed fairly constant within the inner harbour channels until Motuhou Island, from where it amplified slightly to about 0.75 m in the upper reaches of the harbour. The S2 amplitude was also attenuated from 0.096 to 0.086 m (11%) through the harbour entrance, and increased very slightly as it propagated further into the harbour (not shown). The K1 and N2 changed by 1% and 7% respectively across the harbour entrance, and also amplified slightly as they propagated into the harbour. Our modelled predictions for these constituents were also within < 0.01 m of those reported in Mathew (1997) at P1 and P2. The cophase lines in Fig. 5B indicate that the largest phase difference occurred through the confines of the entrance channel followed by a more slowly varying change within the shallower, wider inner basin. Constricted entrances to sub-estuaries (e.g. Te Puna; Fig. 1) also slowed the tidal wave down by approximately 45 minutes.

There were differences in the behaviour of high and low tide that were not captured in the tidal harmonic analysis in Figure 5. The modelled mean water level increased with distance from the entrance of the harbour and this caused the water level at low tide to change by more than the water level at high tide as the wave propagated up the harbour. For example, an increase in the M2 and S2 tidal amplitude from the harbour entrance to Ōmokoroa Point of 5 cm and 2 cm respectively, coupled with a mean water level increase of 5 cm, caused the spring low tide to be only 2 cm lower at Ōmokoroa than at the entrance, whereas the high tide was 12 cm higher. It is very difficult to validate modelled mean water level differences because this requires the water level recorders to be accurately surveyed to the same datum. The amplitude of the M4 tide (the overtide) also increased to about 0.03 m at Ōmokoroa Point, with a phase of 90 degrees relative to the M2 tide (not shown). This caused the time lag between low tide at the harbour entrance and low tide at Ōmokoroa Point to be different for high and low tide. Our model results show this time difference to be in the order of 15 minutes. The phase of the M4 tide (and higher overtides), depends in a complex way on the geometry and the frictional effect of the tidal flats relative to depth of the channels (e.g. Friedrichs & Aubrey 1988), and this delay changes throughout the harbour, and between spring and neap tides. From a practical perspective, this will affect sampling strategies that rely on sampling at a particular stage of the tide, and also will affect predictions for how long and to what extent the tidal flats will be inundated. For example, Tay et al. (2012) show that comparing spatial variations in nutrient concentrations in estuaries is critically dependent on sampling at the same stage of the tide.

Residual currents and residence times

The modelled residual current directions compared relatively well against observations when the current speeds were stronger (giving a maximum error in these cases of c. 60 degrees; Table A2.1). Figure 6 shows the residual current speed modelled for a 28-day period in 2006 coinciding with the FSI deployment (the 'validation simulations') with all available residual current observations (for 1999, 2006 and 2008) superimposed. Residual speeds did not verify overly well against observed residual currents (Table A2.1). However, given that the residual currents represent small differences between large flood and ebb tidal currents, and that the residual current fields vary so much spatially over very short distances, it is difficult to accurately model them. A change of one grid cell in the model can cause a 50% change in the residual current speed, and moving the output model locations by one to two grid cells could improve comparisons considerably. Moreover, the two FSI deployments were in the back eddies on either side of the entrance, where flow conditions were particularly spatially-variable. However, the general pattern of residual circulation shown in the observations was well represented in the model (Fig. 6). For example, the strong ebb-dominated flow along Ōmokoroa Point is modelled, along with flood dominance at the middle

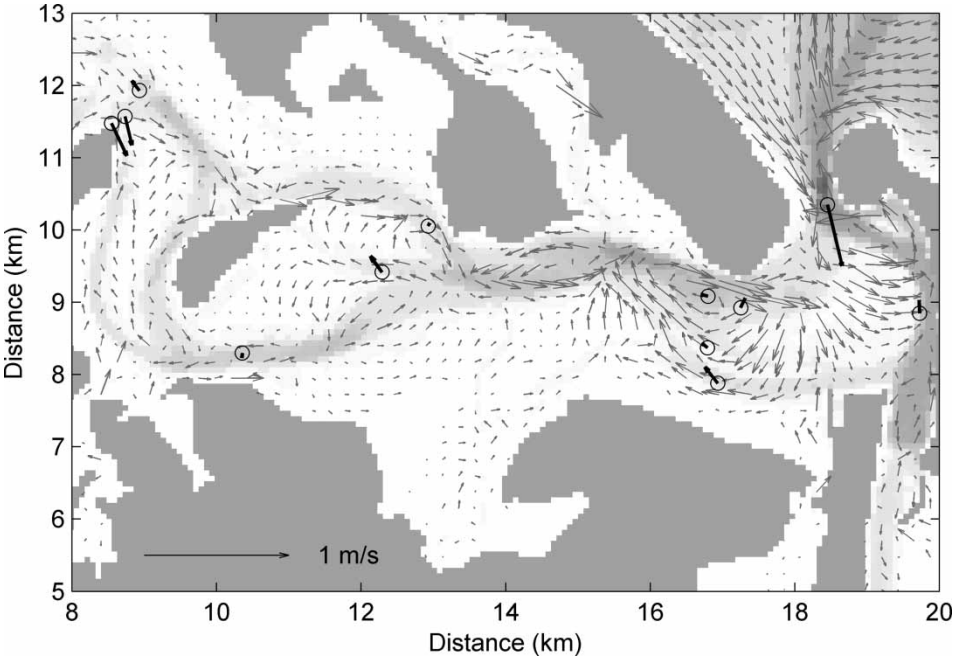

Figure 6 Grey arrows: modelled residual current speed and direction calculated over a 28-day period (the 2006 'validation simulation' period). Solid grey areas indicate dry land and greyscale is water depth. Black arrows with circles: observed residual currents. Note that observed residuals are not measured at the same time or over the same time period as the 28-day model run.

station at Motuhoa (M2), the southern stations at Western (W1) and at the entrance.

With the exception of the main flood tidal delta, the modelled residual currents were relatively low over the tidal flats with greater velocities in the channels (Fig. 6). The residual flow was also relatively low in the sub-estuaries (such as Waikaraeo and Te Puna). In the middle harbour (labelled as Lower Ōmokoroa in Figure 1), there is an ebb-directed flow that runs all the way from Ōmokoroa Point, along the northern part of the harbour along Motuhoa Channel (Fig. 2), and into Western Channel. In the lower harbour (labelled as Deep Channel South in Figure 1), the residual flow is the greatest due to its constricted morphology, and there is evidence of a back-eddy behind Mt Maunganui, and another on the western side of the flood tidal delta. Relatively strong residual currents in the seaward direction were evident immediately seaward of the harbour mouth with the ebb jet eddy dominating the residuals west of the harbour mouth.

The residence time is the average time that a parcel of water spends within a specified region of interest before it departs. ELCOM calculates the residence time of water in each model cell by keeping track of the water age in relation to the rate of exchange of water across the cell boundaries. The harbour was generally well flushed, with modelled residence times of between 2 to 4 days near the harbour mouth and within the Western Channel (Fig. 7). However, the residence times increased by a factor of 2 towards the north end of the basin. Table 3 summarises the modelled average residence times for sub-regions of Tauranga Harbour for windy and calm conditions (scenarios 0–5). Residence times are higher in sub-estuaries with constricted entrances, such as Rangataua Bay and Welcome Bay (Fig. 7C),

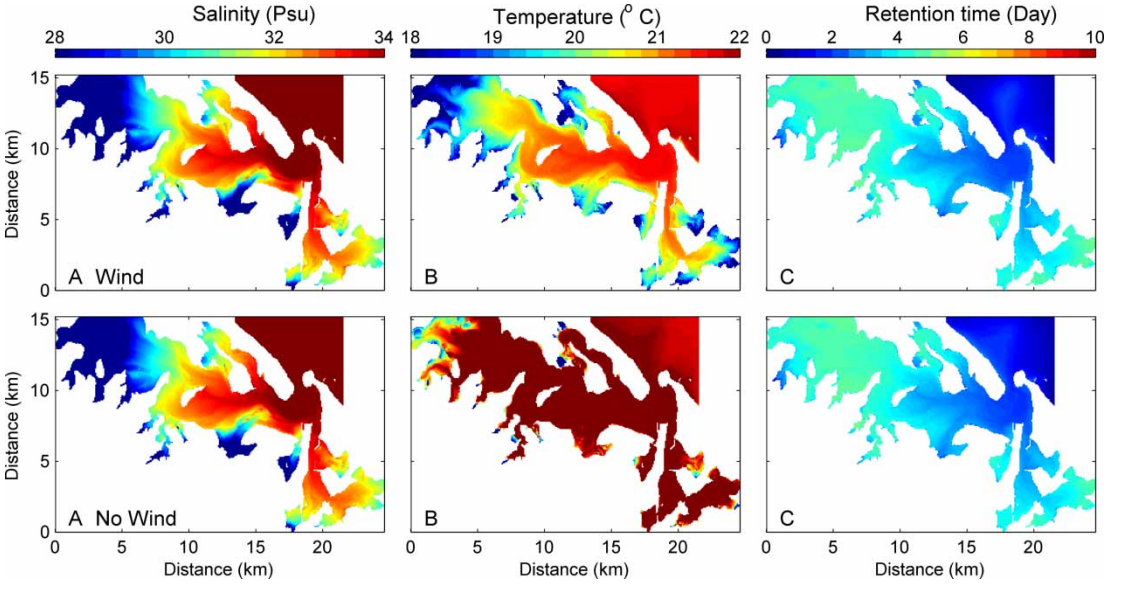

Figure 7 Depth-averaged modelled salinity (A), temperature (B) and residence times (C) of the harbour under dominant wind (top panels) (scenario 0, Table 2) and without wind (bottom panels) conditions for summer (scenario 1, Table 2). The results are averaged over spring to neap tidal conditions (14 days).

with the residence times being some 5 days or so longer than in the main channel. The Deep Channel South (Fig. 1) has lower residence time in part largely due to its depth and close proximity to the entrance, which makes this region the most well-flushed in the harbour. In comparison, Rangataua Bay and Welcome Bay have longer residence times due to their constricted entrances. The Wairoa River mouth is not constricted in comparison; hence, the residence time was lower. Geyer (1997) also found that a shallow estuary with constricted mouth

Table 3 Effect of wind velocity on average residence times of sub-estuaries in the southern basin of Tauranga Harbour.

	Average residence times (day)					
Sub-estuaries division	Scenario 0	Scenario 1	Scenario 2	Scenario 3	Scenario 4	Scenario 5
Waipū Bay	4.8	4.3	2.8	3.2	3.1	3.7
Rangataua Bay	7.8	7.1	3.6	4.1	4.1	5.2
Welcome Bay	8.2	7.4	3.5	4.1	4.0	5.2
Waimapu Estuary	6.4	6.1	4.0	4.8	4.0	4.9
Waikareao Estuary	6.3	5.9	4.6	5.7	4.4	5.4
Wairoa River mouth	4.7	4.3	2.4	3.1	2.6	3.8
Te Puna Estuary	7.4	7.3	6.1	7.9	5.1	6.5
Waikaraka Estuary	7.2	7.0	5.4	6.8	4.6	5.7
Deep Channel South	3.1	2.9	1.7	1.9	2.0	2.4

Note: Refer to Figure 1 for the location of sub-estuaries and Table 2 for scenario conditions.

inhibits wind-induced mixing and increases residence time.

Heath (1976) found that the average residence time of water at Tauranga Harbour to be between 0.8 to 1.5 days based on the tidal prism method. This method gives bulk flushing for a whole estuary or sub-estuary regardless of variation in freshwater inflow, which is an important driving force in estuaries. However, the numerical model results suggest that the irregular geometry and curved channels within the harbour create quiescent side embayments, which increase the residence times compared to the simple shapes that the tidal prism method was developed for. In some areas of the harbour, Heath (1976) averaged results underestimated the residence time by a factor of 4 to 6.

The storm wind conditions (Table 2; scenarios 2–5) reduced the residence time considerably, resulting in (on average across sub-basins) a 39% reduction in residence time for winds in winter and a 24% reduction in summer (Table 3), with wind direction affecting the spatial distribution of residence time and not the average. This was in contrast to the normal wind conditions, which had a minor influence on circulation (compare scenarios 0 and 1; Table 3). Although the average (across all sub-basins) storm residence time was very similar during east and southwesterly winds, there were spatial differences. For example, Te Puna, Waikaraka and Waikaraeo did not experience as strong reduction in residence time as did Welcome Bay, Rangataua and the Wairoa River mouth (Table 3). This could be due to the influence of wind on the Wairoa River (areas strongly influenced by the Wairoa River would have more substantial increases in flushing in the winter when the river flow was higher), or spatial differences in the increase in stream and river inputs during winter. The residual circulation in the central part of the harbour was affected by the direction of the wind during storm events. The most common wind direction is from the southwest, which when strong contributes to a residual ebb current along the southern bank of the estuary, and weakens the northern ebb current (Fig. 8A). This advects the Wairoa River water eastward. Conversely, the same wind speed but with an easterly storm causes an easterly residual flow along the southern bank of the estuary where the water is very shallow. Hence, the easterly wind causes the Wairoa River water to be more quickly flushed from the estuary (Fig. 8B, right panel; also Table 2, 'Wairoa River mouth'), whereas southwesterly winds decrease the residence time of the north ebb-directed residual currents which bring material from the upper estuary to the sea. This indicates that storm sediment and nutrient discharge from the river would more easily be flushed from the estuary during easterly winds.

In summary, the time-averaged modelled residual circulation patterns in Tauranga Harbour showed highly channelised residual currents, with the strongest flow occurring at the harbour mouth and directly out of the harbour mouth. The circulation patterns are likely to affect larval dispersal as in some parts of the harbour, such as in the Ōmokoroa region, the larvae can be retained, while in other areas, such as Wairoa Channel, they would be exported offshore to the shelf environment. The area inwards of Motuhou Channel has a longer residence time compared to the Deep Channel South region and Wairoa River mouth, which would enable retention of food sources for the larvae, and perhaps even serving as a nursery ground for the rest of the harbour. In addition, longer residence times also impact on how quickly sediments and contaminants from the catchment will be flushed out of the sub-compartments of the harbour.

Salinity

The modelled salinity varied spatially across the southern basin of the harbour, with model predictions matching observations to within 0.5 PSU on average. The modelled salinity at the station near the entrance (W2; Fig. 2) was 0.5 PSU too high whereas the modelled salinity higher up the estuary (at station O2) was about 0.5 PSU too low (Fig. 9), with the other stations falling between these two extremes. (The modelled

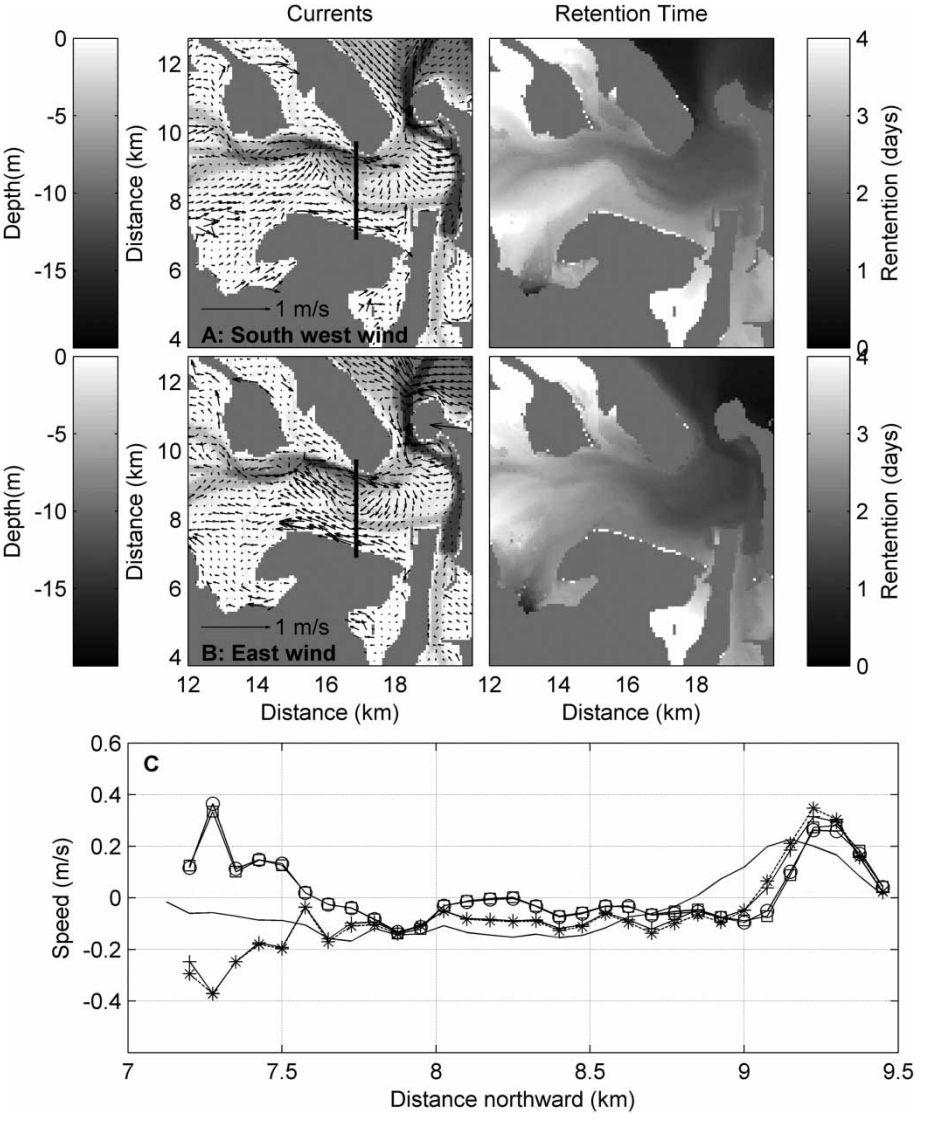

Figure 8 Depth-averaged model results for storm winds over a 14-day spring–neap cycle. Left panels: arrows represent modelled residual current speed and direction. Background greyscale represents the bathymetry. Right panels: modelled retention time. Panel A: wind direction from 250 degrees in winter (scenario 4, Table 2). Panel B: wind direction from 100 degrees in winter (scenario 2). Panel C: east–west current speed at transect marked on upper right panels (— base case (scenario 0); –*– east wind in winter (scenario 2); – + – east wind in summer (scenario 3); –□– west wind in winter (scenario 4); –○– west wind in summer (scenario 5).

salinity was depth-averaged prior to comparison.) A notable deviation was the modelled salinity at Ōmokoroa (Fig. 9) during low tide which was over-predicted by 3 PSU. This could be due to inaccuracies in the Aongatete and Wainui river flows which were estimated from simulated design storm hydrographs rather than using discharge observations. It could also be due to the lack of groundwater inputs in the model, which would have more influence in

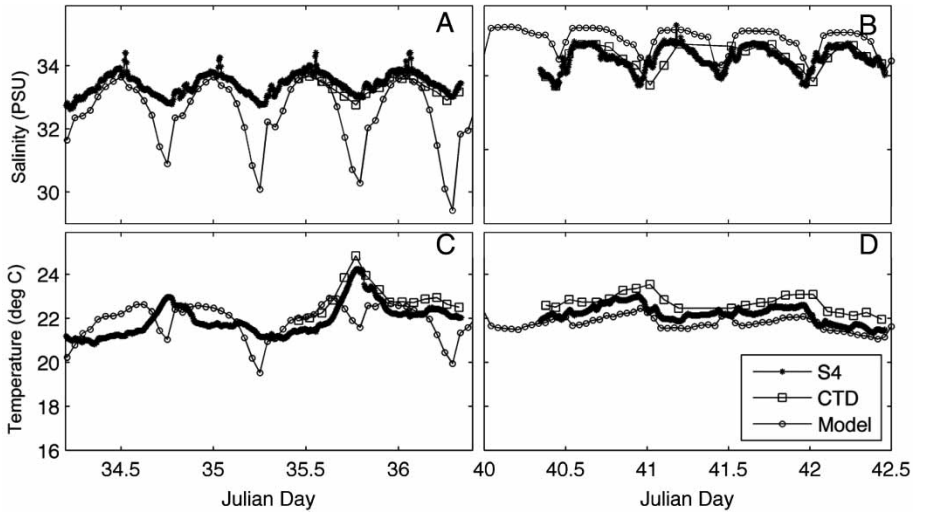

Figure 9 Comparison of measured (S4 and CTD [depth-averaged]) and modelled (ELCOM) salinity and temperature at Ōmokoroa (O2) (A and C) and Western (W2) (B and D) for February 1999. See Figure 2 for station locations.

the higher reaches of the estuary. Obviously, the salinity variation is difficult to reproduce within a numerical model without an accurate understanding of offshore salinity and dilution by various freshwater sources (e.g. groundwater, surface runoff).

Regardless of wind conditions, there was a gradient in salinity between the upper and lower harbour, with three distinct salinity regions: above Ōmokoroa Point; the region between Ōmokoroa Point and Western Channel; and just inside the harbour entrance (Fig. 7A). Higher salinity water was concentrated in the deep channels within the lower harbour. During flood tide, marine water eventually flows over the shallow intertidal regions and, in the first stages of the ebb tide, this water drains off the intertidal flats. However, in the later stages of outgoing tide, the water is confined to the channel. This resulted in higher salinity water within the channels when averaged over all stages of the tide.

Since the year-long CTD dataset for 2001 is collected over much longer time scales than can be reasonably run by the model, rather than verify the absolute salinity over a longer time period we used an approach in which we verified the salinity gradients that were caused by different discharge events. The year-long dataset of biweekly CTD casts at two stations in the upper and lower harbour (C1 and C2; Fig. 2) provided approximately six cases when the Wairoa River had higher than average flow rates (Fig. 10). Other observations were taken when the Wairoa River was at lower (< 20 m^3/s) rates. Unfortunately, the low-flow rates of the river fluctuated significantly in response to hydroelectric dam activity driven by the hourly market electricity prices and the need to regulate supply to compensate for reduced capacity at other stations (W. Bardsley, University of Waikato, pers. comm. 2012). Clearly, salinity variations are unlikely to correlate well with the instantaneous flow rates, so the modelled low-flow rates were smoothed with a 24-hour running mean prior to comparison with the CTD data (Fig. 10A). During high-flow events, excess flood water spills over the dam so flow rates are not affected by the dam. CTD data were depth-averaged and the difference between the two stations correlated well with the Wairoa discharge (Fig. 10C;

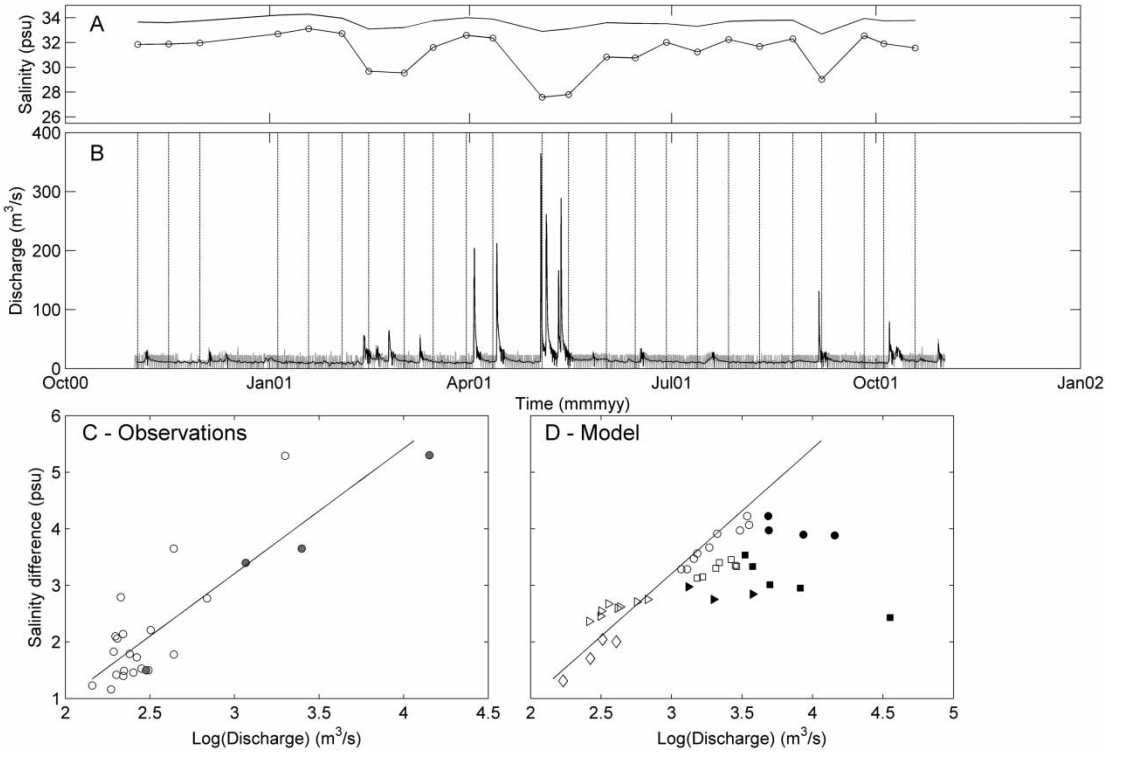

Figure 10 Comparison of the observed salinity variations during 24 different Wairoa discharge levels in 2001 and the modelled salinity variations following three Wairoa discharge events in 2007–2008. Both model and observed salinities have been depth-averaged. Panel A: the depth-averaged salinity observed at Western (C1) (top line with no circles) and Ōmokoroa (C2) stations (bottom line with circles) during 2001. Measurements were collected within approximately 1 hour of high tide (see Figure 2 for station locations). Panel B: discharge in the Wairoa River during 2001. The grey line shows the raw data, the black line has been smoothed with a 24-hour running mean when the discharge was below 20 m^3/s (to smooth the effects of the control exerted by the hydrodams during low flow). Panel C: the relationship between the salinity difference between Western and Ōmokoroa CTD stations and the discharge in the Wairoa River. Filled circles indicate points in which the measurements were collected less than six tidal cycles after a >20 m^3/s discharge event in the Wairoa River. The best-fit line is also plotted ($r^2=0.76$). Panel D: modelled salinity difference between Western and Ōmokoroa stations after the discharge events on 10 December 2007 (41.69 m^3/s, triangles), 8 September 2008, (175.9 m^3/s, circles), 16 August 2008 (63.69 m^3/s, squares). The diamonds indicate the low-flow conditions modelled prior to each of these three events and the February 2008 scenario used in Figure 7. The multiple symbols indicate each successive high tide following the event, with the filled squares indicating the tides immediately following the highest discharge.

$r^2=0.76$, although the data were not normally distributed despite log-transforming the discharge rates). This best-fit line provided a baseline against which to benchmark the model results (Fig. 10D). Modelled low-flow conditions fitted well to this line (diamonds in Figure 10D). Modelled salinity differences were less than measured for the three discharge events tested (circles, triangles and squares in Figure 10D). However, the CTD data were collected at varying numbers of tidal cycles from the event. The filled circles in Figure 10C show the only observations that were collected within 6 hours of a discharge event. Model results consistently approach the line as the number of tidal cycles after the event increases.

One event exactly asymptotes onto the line (8 September 2008), one below (16 August 2008) and one above (10 December 2007).

To examine the detailed influence of the extreme freshwater inflow event (scenario 6; Table 2) from the head of Wairoa River mouth where it enters the estuary, we extracted a 'vertical profile' from the model stretching from the river mouth to the harbour entrance (Fig. 11), in order to provide a profile of any freshwater plume that may develop. The Wairoa River input caused a stratified water column that gradually became more and more vertically well-mixed with distance from the river mouth (Fig. 12). Under low-flow conditions prior to the event (1 April 2008), the maximum difference over a tidal cycle across the halocline was 13 PSU. The surface horizontal salinity front (defined as the maximum surface salinity gradient) occurred 3 km from the mouth of the Wairoa River. During the high discharge event (15 April 2008), the salinity front moved towards the harbour entrance, resulting in a reduction in depth-averaged salinity at the river mouth by 5 PSU, and an overall reduction in salinity of the whole harbour by 3 to 5 PSU. Furthermore, the difference across the halocline increased to 14. The average harbour temperature dropped 1 °C, while within the main plume the temperature fell by 4 °C when the river was in flood (Fig. 12B, D). Although the river temperature was the same between scenarios, the open boundary temperature was slightly colder. The average wind speed was at 2.3 m/s during the low-flow conditions and at 6.6 m/s during the high discharge event.

The model showed that the periodic flooding events caused variations in salinity and temperature structure of the harbour associated with the increased development of a freshwater plume. Comparison with observations of salinity differences between the entrance and Ōmokoroa collected using the CTD (C1 and C2, Fig. 2) indicate that the modelled salinity differences caused by this discharge event are probably not great enough. This could be attributed to neglecting freshwater sources such as groundwater and direct runoff. Figure 10A clearly shows a seasonality to the observations, with the early spring salinity differences being greater than late summer in cases when the river was in a low-flow state for a number of weeks. Not only is this seasonality not well captured in the open ocean conditions, it is also probably not well captured in the start-up model conditions, which were always initialised in the same way. In all cases, 7–8 days were modelled prior to the discharge event, but this will probably not be enough to cause a seasonal change to the overall distribution of salinity within the harbour. If only the observations that were taken within six tidal cycles of the

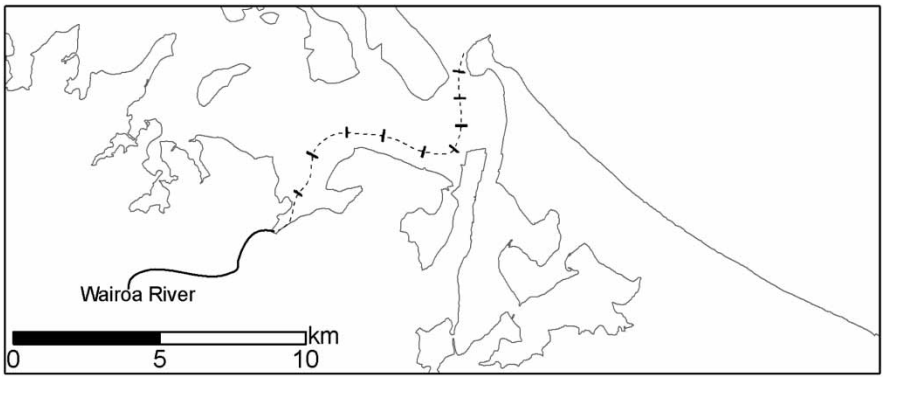

Figure 11 The dashed line represents the vertical profile extracted from model output that begins at Tauranga Harbour southern basin entrance and ends at Wairoa River mouth and runs along the main channel. The orthogonal black lines mark each 1000 m.

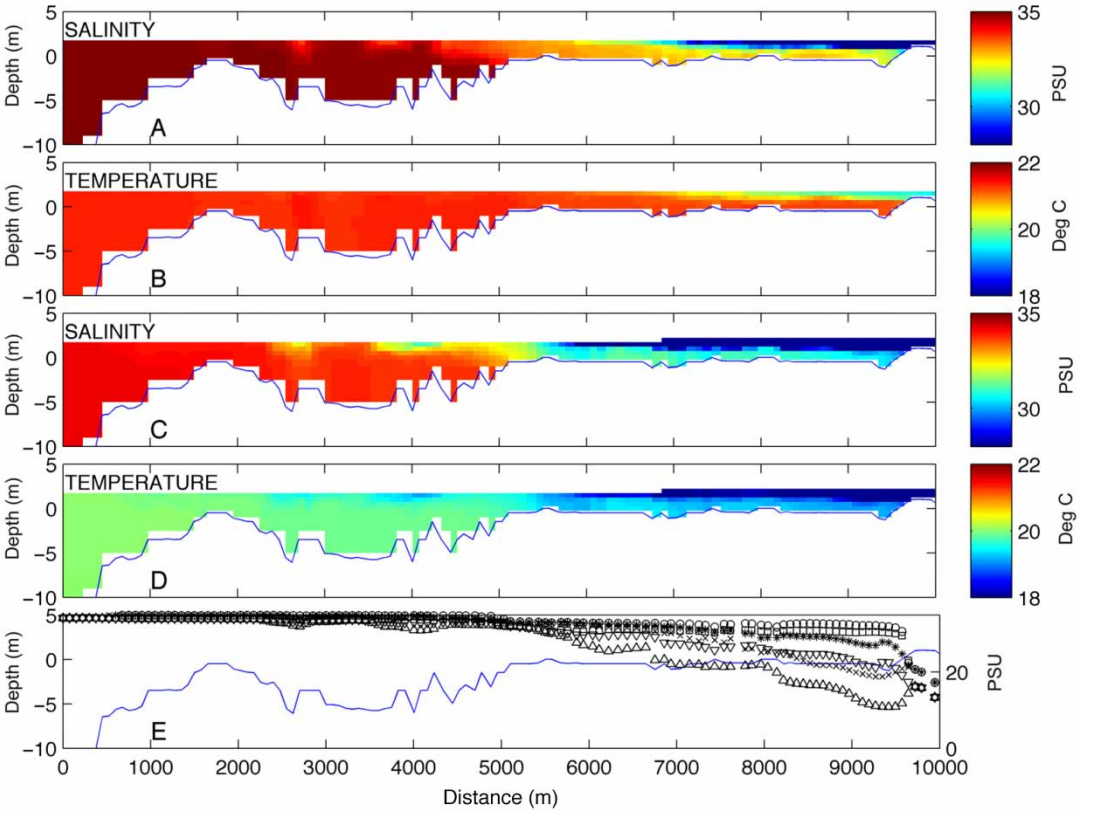

Figure 12 Tidal average of salinity and temperature in the harbour along a vertical profile extracted from the model extending landward from the harbour mouth (0 m at Mt Maunganui entrance) to Wairoa River (9825 m), (A and B) under normal flow conditions, 1 April 2008, (C and D) when the 539.9 m^3/s Wairoa River discharge event occurred on 15 April 2008 (scenario 6, Table 2). Panel E shows the depth-averaged maximum, minimum and average salinity during normal flow and the extreme discharge event. The markers o,*, x represent, respectively, the depth-averaged maximum, average and minimum salinity during normal flow. The markers □, △, ▽ represent, respectively, the depth-averaged maximum, average and minimum salinity during the extreme discharge event.

discharge event are considered (grey circles in Fig. 10C), the points lie more along the line. This is an indication that the model is better at predicting the effects of quick-flow into the harbour, but the effect of base-flow freshwater input would need far better characterisation of groundwater. Figure 10D shows that it takes approximately three to five tidal cycles for freshwater to be mixed into the estuary and the estuary salinity gradient to be influenced by the pulse of freshwater.

Bivalve mollusc species that are dominant in Tauranga Harbour, such as *Paphies australis*, are sensitive to an altered salinity regime. McLeod and Wing (2008) demonstrated that bivalves (*Austrovenus stutchburyi* and *Paphies australis*) were smaller in river deltas near the outflow of a power station in Doubtful Sound, and with sustained exposure ($>$ 30 days) to low salinity ($<$ 10 PSU) bivalve survivorship significantly decreased. However, the bivalves can sustain periods of exposure to freshwater of at least 20 days if followed by a period of normal seawater salinity. The extreme discharge event modelled here altered the salinity structure more from the river mouth to 6 km

away from the river mouth. This salinity environment may restrict bivalves to the deeper water in the channel (McLeod & Wing 2008). McLeod and Wing (2008) examined salinity structure at Doubtful Sound in light of their laboratory experiments and found that bivalves are restricted to deeper water (5–6 m depth). However, it is also possible this deeper water may experience reduced oxygen levels during discharge events. Considering the Wairoa River part of the estuary, its ratio of river discharge over a tidal cycle ($R = 20\ m^3/s \times (12.4 \times 3600)$ s) to volume of water entering the estuary on a flood tide ($V = 5{,}400{,}000\ m^2 \times 1.2$ m) gives an R/V ratio of 0.14 which makes this part of the estuary partially mixed. When the discharge increases to 540 m^3/s, this part of the estuary becomes highly stratified with an R/V of 3.7, conditions which can lead to eutrophication issues (e.g. Christian et al. 1991) if sustained. This would equate to a change from category F to category C around the river mouth region using the Hume et al. (2007) classification. However, our model results show that these conditions are likely dissipated within a week to 10 days following the event. For example, in the cases we modelled, it took from four to five tidal cycles for the Wairoa-related salinity differences to trend downwards, at which point they trended downwards at a rate of 0.25–0.5 PSU per tidal cycle (Fig. 10C).

Temperature

The model generally reproduced the temperature variations well. For example, at Western, the modelled variation in temperature was consistent with the measured water temperature; although being between 1–2 °C lower than temperature measured by the S4 and CTD (Fig. 9). However, at Ōmokoroa, the measured temperature showed an increase in temperature during the late afternoon low tide that the model did not capture, which ultimately led to a difference in temperature of 3 °C during afternoon and evening ebb tides.

The temperature structure within the harbour is very sensitive to wind mixing, as seen in Figure 7B. Calm conditions resulted in warmer temperatures throughout the harbour, with temperature generally > 22 °C, while wind conditions resulted in a decrease in water temperature with a range between 18 to 22 °C in various parts of the harbour. There are two ways that the wind can change the water temperature in the model. Firstly, the energy heat transfer at the surface due to radiative transfer, and evaporative and sensible (conduction and convection) heat loss, can change the heat content of the water. The latter two are both modelled with an equation that depends on the wind speed. Secondly, enhanced mixing between layers is caused by the wind, thus increasing the surface current speed, which will exchange heat more effectively from lower layers in the model. Heat is absorbed by each layer in the water column, and converted in the model to a change in temperature within that layer. The bulk extinction coefficient determines how quickly the heat is absorbed, and is set so that the energy is absorbed within the first metre of the water column. If the depth is less than a metre, the heat not absorbed in the water column is assumed to heat the sediments.

The under-prediction of water temperature at Ōmokoroa (Fig. 9) was generally caused by poor predictions of the temperature of late afternoon ebb tides in the upper estuary. Measured (S4 and CTD) temperature data displayed a diurnal signal at this station that, although successfully reproduced at other stations, was not reproduced well here. The higher water temperatures observed for late afternoon ebb tides at Ōmokoroa could be due to the heating of the shallow tidal flat area by solar radiation during the preceding low tide period, which then heats the water during the flood tide. During the next ebb tide the heated water passes by the measuring station at Ōmokoroa Point. During the later stages of outgoing tide, the lowered water level causes the water to be confined to the channels which are deeper and do not heat up as much as the shallow regions.

The model does not include any heating of intertidal sediments when they are exposed. Harrison and Phizacklea (1987a) observed rapid changes of intertidal sediment temperature during tidal inundation. Increasing water temperature in summer, along with anoxic conditions in the sediment, may accelerate nutrient release from the sediment which, in turn, raises the eutrophication level. Higher temperatures in summer tend to increase ammonium regeneration rates and pore-water concentrations (Nixon 1981) which may result in summer nitrification maxima. This late afternoon ebb-flow warming was also observed in 24-hour CTD casts taken at the mouth of Te Puna and Waikareao Estuaries, in summer and spring (Tay et al. 2012).

ELCOM uses a fixed water albedo in calculating the heat exchange between air and water, but in estuaries with extensive tidal flats the surface tidal flat albedo has been shown to change as a function of the periodic exposure to solar radiation caused by the tidal cycle (Kim et al. 2007). Sediment has been shown to be important for heat exchanges in rivers where it accounted for 15% of the observed energy exchange in a study conducted at the River Blithe in the UK (Evans et al. 1998). The study showed that reflected short-wave radiation from the bed caused the majority of the measured bed heat flux, which overwhelmed long-wave radiation from the sediments. In ELCOM, any excess of short-wave energy at the bottom water column is reflected back into the domain. An investigation at Pāuatahanui Inlet, New Zealand, based on 24 hours of data, concluded that benthic heat exchanges were relatively small compared with surface and horizontal exchanges in the water column (Heath 1977). However, investigations in Scotland demonstrated that the temperature gradient of exposed sediments can undergo a noticeable change as the tide floods over the shore, and it has been suggested that rapid heat exchange occurs between the intertidal sediments and incoming tidal water (Harrison & Phizacklea 1987a, b).

Another cause of the mismatch in modelled and observed temperature in water draining from the intertidal sandflats may be that the air temperature over the intertidal flats differs considerably from that used in the model. The meteorological boundary conditions for the model were sourced from Tauranga Airport (c. 14 km from Ōmokoroa). The average February 2008 air temperature measured at the Ōtūmoetai weather station, which is situated close to Waikareao Estuary, was 1.6 °C higher than the airport air temperature. The weather station located at the airport is in a flat urban setting while the area around Ōmokoroa is in a rural setting with steeper topography, so that the wind conditions on the sandflats near Ōmokoroa might also be quite different than the wind conditions used in the model. In particular, the wind speed used in the model was higher during the late afternoon in summer and spring simulations. These strong winds are effective at extracting heat from shallow areas through evaporation and enhanced mixing (as shown in Figure 9A), and so might remove too much heat from the water over the intertidal sandflats. Therefore, incorporating spatially-varying weather conditions in the model might improve simulations in the upper estuary.

Conclusion

A 3-D hydrodynamic model, complemented by field data, was used to characterise circulation, temperature and salinity patterns in the southern basin of Tauranga Harbour. The model has established that there is a weak salinity gradient in the harbour which is modulated by tidal variations. This gradient strengthens dramatically when high freshwater discharge events occur, which are largely controlled by the input from the Wairoa River. Conversely, the temperature profiles tend to vary diurnally rather than tidally, and are sensitive to the strength of the wind. Wind-driven circulation reduces the temperature, especially of the tidal flat areas, by 2–4 °C in the upper parts of the harbour. The residence times varied across the harbour with low residence times in the mouth of the

harbour and in sub-estuaries that are well exposed to tidal currents (Wairoa River). The residence times were high in sub-estuaries with constricted entrances and also increased with distance from the harbour entrance, making these areas more susceptible to accumulation of sediments and contaminants. Periodic freshwater discharge events in the Wairoa River can decrease the salinity and temperature more than 5 km away from the river mouth, causing a change to the vertical structure of the estuary around the river mouth, which could affect the ecological condition of the harbour, albeit temporarily.

Acknowledgements

We would like to acknowledge Bay of Plenty Regional Council (BOPRC) who provided river discharge measurements and, in particular, Glenn Ellery who provided insight into Wairoa River discharge measurements. Port of Tauranga Ltd provided water level and ADCP data. Dudley Bell, Hilke Giles and Helen Kettles assisted in the collection of field data and Brett Beamsley helped construct the bathymetric grid. Kate Giles (CTD measurements) and Kyle Spiers, both from the University of Waikato, provided field data for model calibration/validation. This paper is dedicated to the memory of Professor Terry Healy, University of Waikato, who contributed immensely to our understanding of Tauranga Harbour, and who passed away in 2010.

References

Abrahim G, Parker R 2002. Heavy-metal contaminants in Tamaki Estuary: impact of city development and growth, Auckland, New Zealand. Environmental Geology 42: 883–890.

Barnett A 1985. Tauranga Harbour study: a report for the Bay of Plenty Board. Part I: overview; Part III: hydrodynamics. New Zealand Ministry of Works and Development. 74 p.

Beca Carter Hollings and Ferner Ltd 1999. Guidelines for stormwater runoff modelling in the Auckland Region. Technical Report 108. 26 p.

Black K 1984. Tauranga Harbour study: a report for the Bay of Plenty Board. Part IV: sediment transport. New Zealand Ministry of Works and Development. 159 p.

Chagué-Goff C, Nichol SL, Jenkinson AV, Heijnis H 2000. Signatures of natural catastrophic events and anthropogenic impact in an estuarine environment, New Zealand. Marine Geology 167: 285–301.

Christian RR, Boyer JN, Stanley DW 1991. Multiyear distribution patterns of nutrients within the Neuse River Estuary, North Carolina. Marine Ecology Progress Series 71: 259–274.

Cole RG, Hull PJ, Healy TR 2000. Assemblage structure, spatial patterns, recruitment, and post-settlement mortality of subtidal bivalve molluscs in a large harbour in north-eastern New Zealand. New Zealand Journal of Marine and Freshwater Research 34: 317–329.

Davies-Colley RJ, Healy TR 1978. Sediment and hydrodynamics of the Tauranga entrance to Tauranga Harbour. New Zealand Journal of Marine and Freshwater Research 12: 225–236.

de Lange WP 1988. Wave climate and sediment transport within Tauranga Harbour, in the vicinity of Pilot Bay. Unpublished PhD thesis. Hamilton, New Zealand, University of Waikato. 189 p.

Evans EC, McGregor GR, Petts GE 1998. River energy budgets with special reference to river bed processes. Hydrological Processes 12: 575–595.

Friedrichs CT, Aubrey DG 1988. Non-linear tidal distortions in shallow well-mixed estuaries: a synthesis. Estuarine, Coastal and Shelf Science 27: 521–545.

Geyer WR 1997. Influence of wind on dynamics and flushing of shallow estuaries. Estuarine, Coastal and Shelf Sciences 44: 713–722.

Giles KF 2002. Seasonal dynamics of zooplankton in Tauranga Harbour, New Zealand. Unpublished MSc thesis. Hamilton, New Zealand, University of Waikato. 109 p.

Hansen DV, Rattray M 1966. New dimensions in estuary classification. Limnology and Oceanography 3: 319–326.

Harrison SJ, Phizacklea AP 1987a. Temperature fluctuation in muddy intertidal sediments, Forth Estuary, Scotland. Estuarine, Coastal and Shelf Science 24: 279–288.

Harrison SJ, Phizacklea AP 1987b. Vertical temperature gradients in muddy intertidal sediments in the Forth Estuary, Scotland. Limnology and Oceanography 32: 954–963.

Healy TR 1985. Tauranga Harbour study: a report for the Bay of Plenty Board. Part II: field data collection programme; Part V: morphological study. New Zealand Ministry of Works and Development. 25 p.

Healy TR, Black KP, de Lange WP 1987. Field investigations required for numerical model studies of port developments in tidal inlet harbours. In: Gardiner V ed. International geomorphology 1986. London, John Wiley and Sons. Pp. 1099–1112.

Healy TR, Bell R, de Lange WP 1993. Predicting morphodynamic change from tidal residual vectors at a large tidal inlet, Tauranga Harbour, New Zealand. In: List JH ed. Large scale coastal behaviour '93, volume 1. St Petersburg, FL, US Geological Survey Open File Report 93-381. Pp. 64–67.

Healy TR, Kirk RM 1992. Coasts. In: Soons JM, Selby MJ eds. Landforms of New Zealand. 2nd edition. Auckland, New Zealand, Longman Paul Ltd. Pp. 81–104.

Heath RA 1976. Broad classification of New Zealand inlets with emphasis on residence times. New Zealand Journal of Marine and Freshwater Research 10: 429–444.

Heath RA 1977. Heat balance in a small coastal inlet Pāuatahanui Inlet, North Island, New Zealand. Estuarine and Coastal Marine Science 5: 783–792.

Hodges BR, Imberger J, Saggio A, Winters KB 2000. Modelling basin scale waves in a stratified lake. Limnology and Oceanography 45: 1603–1620.

Hodges BR, Dallimore C 2006. Estuary and Lake Computer Model: ELCOM science manual version 2.2. Perth, Centre for Water Research, University of Western Australia. 52 p.

Hume TM, Green MO, Elliott S 2009. Tauranga Harbour sediment study: assessment of predictions for management. NIWA Client Report HAM2009-139 December 2009 for Environment Bay of Plenty. 124 p.

Hume TM, Snelder T, Weatherhead M, Liefting R 2007. A controlling factor approach to estuary classification. Ocean and Coastal Management 50: 905–929.

Kim T-W, Cho Y-K, Dever EP 2007. An evaluation of the thermal properties and albedo of a macrotidal flat. Journal of Geophysical Research 112, C12009. doi:10.1029/2006JC004015

Mathew J 1997. Morphologic changes of tidal deltas and an inner shelf dump ground from large scale dredging and dumping, Tauranga, New Zealand. Unpublished PhD thesis. Hamilton, New Zealand, University of Waikato. 351 p.

McLeod RJ, Wing SR 2008. Influence of an altered salinity regime on the population structure of two infaunal bivalve species. Estuarine Coastal and Shelf Science 78: 529–540.

Nixon SW 1981. Remineralization and nutrient cycling in coastal marine ecosystems. In: Neilson BJ, Cronin LE eds. Estuaries and nutrients. Totowa, NJ, Humana Press. Pp. 111–138.

Oldman JW, Black KP, Swales A, Stroud MJ 2009. Prediction of annual average sedimentation rates in an estuary using numerical models with verification against core data-Mahurangi Estuary, New Zealand. Estuarine, Coastal and Shelf Science 84: 483–492.

Park S 2004. Aspects of mangrove distribution and abundance in Tauranga Harbour. Environmental publication 2004/16. Whakatāne, New Zealand, Environment Bay of Plenty. 40 p.

Park S 2005. Bay of Plenty coastal water quality 2003–2004. Report No. 2005/13. Whakatāne, New Zealand, Environment Bay of Plenty. 86 p.

Pawlowicz R, Beardsley B, Lentz S 2002. Classical tidal harmonic analysis including error estimates in MATLAB using T_TIDE. Computers and Geosciences 28: 929–937.

Rabouille C, Conley DJ, Dai MH, Cai W-J, Chen CTA, Lansard B, Green R, Yin K, Harrison PJ, Dagg M, McKee B 2008. Comparison of hypoxia among four river-dominated ocean margins: the Changjiang (Yangtze), Mississippi, Pearl and Rhône Rivers. Continental Shelf Research 28: 1527–1537.

Scholes P, Greening G, Campbell D, Sim J, Gibbons-Davies J, Dohnt G, Hill K, Kruis I, Shoemack P, Davis A 2009. Microbiological quality of shellfish in estuarine areas: Joint agency research report. Bay of Plenty Regional Council, Institute of Environmental Science and Research, New Zealand Food Safety Authority, Tauranga City Council, Western Bay of Plenty District Council and Toi Te Ora – Public Health. 89 p.

SCS (Soil Conservation Service) 1972. SCS national engineering handbook: hydrology. Washington, DC, US Government Printing Office.

SCS (Soil Conservation Service) 1975. United States Department of Agriculture, Soil Conservation Service technical release no. 55: Urban hydrology for small watersheds. Washington, DC, Engineering Division, SCS, US Department of Agriculture.

Spiers KC, Healy TR, Winter C 2009. Ebb-jet dynamics and transient eddy formation at Tauranga Harbour: implications for entrance channel shoaling. Journal of Coastal Research 25: 234–247.

Tay HW, Bryan KR, Pilditch CA, Park S, Hamilton DP 2012. Variations in nutrient concentrations at different time scales in two shallow tidally dominated estuaries. Marine and Freshwater Research 63: 95–109.

Vennell R 2006. ADCP measurements of momentum balance and dynamic topography in a constricted tidal channel. Journal of Physical Oceanography 36: 177–188.

Appendix 1

Table A1.1 Summary of tidal elevation and phase calibration (c) and validation (v) results.

Station	Calibration/ validation	MAE (m)	RMS error (m)	M2 amp error (m)	M2 phase error (degrees)	N2 amp error (m)	N2 phase error (degrees)	S2 amp error (m)	S2 phase error (degrees)	K1 amp error (m)	K1 phase error (degrees)
O1	C	0.21	0.24	0.15	8.09	–	–	–	–	–	–
M1	C	0.16	0.18	0.08	3.38	–	–	–	–	–	–
W1	C	0.12	0.14	0.02	1.61	–	–	–	–	–	–
F1	V	0.07	0.08	0.04	1.91	0.01	0.90	0.01	1.77	0.04	2.76
F2	V	0.07	0.08	0.03	0.09	0.01	2.29	0.01	3.34	0.04	2.16
P1	V	0.08	0.12	0.03	1.62	0.00	2.38	0.00	2.50	0.05	3.95
P2	V	0.10	0.16	0.04	0.58	0.00	7.23	0.02	5.44	0.05	1.11
B1	V	0.09	0.19	0.07	6.11	0.02	8.46	0.01	8.48	0.04	6.31
B2	V	0.15	0.17	0.04	8.36	0.02	38.16	0.03	2.86	0.04	4.97

Notes: Site locations are marked on Figure 2; MAE is mean absolute error; RMS is root mean square error.

Appendix 2

Table A2.1 Summary of current speed and direction calibration (c) and validation (v) results.

		Total			Flood			Ebb			Residual	
		Speed (m/s)		Direction (degrees)	Speed (m/s)		Direction (degrees)	Speed (m/s)		Direction (degrees)	Speed (m/s)	Direction (degrees)
Station	Calibration/ validation	MAE	RMS	MAE	MAE	RMS	MAE	MAE	RMS	MAE	MAE	MAE
O1	C	0.18	0.22	22.05	0.46	0.18	35.80	0.60	0.17	8.30	0.13	36.15
O2	C	0.14	0.17	5.77	0.07	0.09	7.05	0.17	0.18	4.49	0.07	18.62
O3	C	0.12	0.14	0.87	0.11	0.13	8.26	0.08	0.10	10.00	0.02	182.75
M1	C	0.10	0.13	5.97	0.46	0.11	6.45	0.56	0.11	5.49	0.03	22.79
M2	C	0.12	0.15	8.00	0.10	0.12	15.90	0.07	0.08	0.09	0.07	62.96
M3	C	0.14	0.16	5.56	0.16	0.18	9.95	0.10	0.11	1.16	0.03	143.67
W1	C	0.08	0.10	15.45	0.38	0.12	9.50	0.36	0.06	21.40	0.02	26.03
W2	C	0.08	0.10	6.18	0.10	0.12	4.76	0.12	0.15	7.60	0.05	9.08
W3	C	0.02	0.15	10.55	0.15	0.16	15.60	0.05	0.06	5.50	0.05	84.41
F1	V	0.14	0.18	13.40	0.14	0.17	8.50	0.17	0.19	18.30	0.01	154.53
F2	V	0.10	0.12	2.91	0.12	0.13	5.27	0.08	0.10	−0.54	0.02	13.85
A	V	0.15	0.18	24.00	0.16	0.20	38.00	0.15	0.17	10.00	0.24	19.78

Notes: Site locations are marked on Figure 2; MAE is mean absolute error; RMS is root mean square error. The mean flood and ebb direction were evaluated when the tide flows had stabilised, and the mean direction is the mean of the ebb and flood directions.